

# Denoising of Electron Tomographic Reconstructions from Biological Specimens Using Multidimensional Multiscale Transforms

Arne Stoschek<sup>1</sup>, Thomas P.Y. Yu<sup>2</sup>, and Reiner Hegerl<sup>1</sup>

(1) Max-Planck-Institute for Biochemistry, D-82152 Martinsried b. München, Germany

(2) Stanford University, Department of Computer Science, SCCM, Stanford, CA 94305, USA

Email: stoschek@biochem.mpg.de, pyu@sccm.stanford.edu, hegerl@biochem.mpg.de

## ABSTRACT

*In electron tomographic reconstructions of biological specimens the information about their structure is not directly accessible since most of the signal is buried in noise. An interpretation of the images using surface and volume rendering techniques is difficult due to the noise sensitivity of rendering algorithms. We explore the use of various multiscale representations for denoising 2D and 3D images. Orthogonal wavelet transforms applied to multidimensional data exhibit poor results due to the lack of translational and directional invariance. Extending the 1D translation-invariant denoising algorithm of Coifman and Donoho to higher dimensions proves to overcome the poor performance of orthogonal wavelet transforms. We present a method to quantify the loss of information due to denoising artifacts on data with an unknown signal-noise relationship, and propose a scheme for denoising of such data. Experiments show invariant wavelet denoising to perform well in reconstructing signals out of noisy 3D data while preserving most of the actual information.*

## 1. INTRODUCTION

Direct imaging of biological specimens (e.g. macromolecular assemblies or cellular sections) using transmission electron microscopy is a powerful tool in structural molecular biology. In good approximation, the obtained images are 2D projections of densities from the imaged volume. By means of techniques similar to medical computed tomography, it is possible to reveal the true 3D information (e.g. tomographic reconstruction [7]). Although electron microscopes are able to image biological objects with a resolution down to 0.3 nm, the structural information is not directly accessible since most of the signal is buried in noise (SNR  $\approx$  0 dB). An interpretation of the images using surface and volume rendering techniques is difficult due to the noise sensitivity of rendering algorithms. A denoising algorithm that is suitable for our application must be able to preserve as much as possible of the signal while reducing the noise to a sufficiently low level. We demonstrate the applicability of the invariant wavelet representation in reconstructing signal out of noisy 3D data with an unknown signal-noise relationship.

## 2. MULTISCALE TRANSFORM BASED DENOISING

A basic algorithm for denoising is to apply a suitable signal transform to the noisy data, then applying some thresholding scheme in the transform domain (thereby suppressing coefficients smaller than a certain amplitude), and finally inverting the transform. Denoising based on wavelets has proven to be a suitable method for 1D signals [2]. However, a straightforward extension to multidimensional data gives very poor results due to the lack of translational and directional invariance of orthogonal wavelet transforms. Denoising artifacts are intimately connected with the location and orientation of discontinuities in the signal space. One approach [1] in order to correct misalignments between features of the signal and of the wavelet basis function is to apply a range of shifts to the signal (i.e. changing the feature positions) and average over the obtained result (*cycle spinning*). In a higher-dimensional signal space this shift can be translational or rotational (or a combination of both). We denote the noisy data to be  $x$ ,  $T$  is the denoising operator,  $S_\Delta$  is the translational/rotational shift operator referring to all discrete values belonging to the translational/rotational degrees of freedom  $\Delta$  in the signal space. Thus, the invariant denoising operator is

$$\bar{T}(x; S_\Delta) = \text{Ave}[S_{-\Delta}(T(S_\Delta x))]. \quad (1)$$

Although a naive implementation of this operator would be very impractical as for the computational costs, extending the fast 1D-algorithm of [1] to higher dimensions reduces the costs considerably.

Another approach to improve on orthogonal wavelet transform in 2D is the steerable pyramid [3]. This representation is an overcomplete, multiscale, and multi-orientation transform with the property being jointly translation- and direction-invariant in a weak sense. Although computationally very efficient in 2D, an extension of the steerable pyramid for higher dimensions seems to be quite difficult due to the iterative optimization procedure used to synthesize the basis functions.

We decide for the modification of the coefficients to utilize the soft-thresholding function

$$y = \text{sign}(x) \cdot (|x| - \lambda) \quad (2)$$

with  $y = 0$  for  $|x| < \lambda$  as proposed in [2]. Every individual subband (for the steerable pyramid every oriented subband) is thresholded with a different threshold value  $\lambda$ . An optimum choice of the threshold depends on the exact knowledge of the spectral signal-to-noise relationship which is not available for our type of imagery. Instead, we choose to shrink the subbands by a certain quantile of the bands. We find that soft-thresholding by the median value (50% quantile) gives very acceptable results. The choice of the median is motivated by the fact that an appropriate multiscale transform can efficiently compress the signal into a small number of significantly large coefficients, whereas noise spreads out as small coefficients in each band. Thresholding by the median value is robust in terms of keeping the large coefficients (i.e. the signal) while considerably reducing the noise power.

### 3. TEST RESULTS

A widely used method for signal reconstruction in electron microscopy images is to average over a large number of redundant structures, thus reducing the additive image noise. We assume the averaging to be an ideal denoising procedure, i. e. causing no denoising artifacts. In the following we utilize a statistical method to evaluate the quality of denoising when applied on redundant structures in order to infer to the quality on unique, non-repeatable structures. To quantify the spectral dependency of denoising artifacts when using multiscale transforms we employ the radial correlation function (RCF) [5], also called Fourier ring correlation. The RCF compares two statistically independent averages from the original ( $f_o$ ) and denoised data ( $f_d$ ) by inspecting their Fourier coefficients along rings in the Fourier space. A normalized sum from the complex multiplication of the spatial coefficients along individual rings is calculated and plotted against the corresponding spatial frequency  $\omega$ :

$$RCF(\omega) = \frac{\sum_{\omega} (F_o \cdot F_d^*)}{\sqrt{\sum_{\omega} |F_o|^2 \cdot \sum_{\omega} |F_d|^2}} \quad (3)$$

with  $F = \mathbf{FT}\{f\}$  and  $F^*$  denoting the complex conjugate of  $F$ .

The determination of the denoising artifacts was carried out on 2D electron microscope images containing 3096 characteristic views of one type of molecule (see Fig. 1-left). The averaging requires mutual alignment of the objects with respect to rotation and translation. The alignment of the denoised data refers to the alignment parameters as obtained from the original data (this ensures independence from possible denoising artifacts). The radial correlation function from the original data reflects the transmission of the used electron microscope over the relative frequency. Fig. 1 (right) shows the considerable deviations in the radial correlation functions between original and orthogonal wavelet denoised data. Steerable

pyramid denoising as well as translation- and rotation-invariant denoising [4] performs much better. However, the computational costs of the latter are considerably higher. When comparing soft and hard thresholding [2] we observe soft thresholding to be much better in removing noise compared to hard thresholding while keeping the same amount of signal.

We attempt to denoise 3D data by two means: (i) slide-by-slide pseudo-3D denoising and (ii) denoising based on a full 3D transform. We apply denoising to synthetic test data as well as to three-dimensionally reconstructed volumes of unique, non-repeatable structures obtained by electron tomography [6]. Due to the limited tilt angle ( $\pm 60^\circ$ ) of the electron microscope, the tomographic reconstruction has an orientation-dependent information content (a limited information in z-direction). In order to quantify the effect of denoising synthetic 3D-data we defined three measures: (i) noise reduction as the ratio of the standard deviations of the noise between noisy and denoised data, (ii) mean square error between original (noise-free) and denoised data, and (iii) cross-correlation coefficient between original and denoised data. The results of the tests are given in Table 1 as well as in Fig. 3. For the 3D denoising we observe the truly 3D invariant anisotropic wavelet representation [4] (Fig. 3g) to outperform the pseudo-3D steerable pyramid representation (Fig. 3f). Orthogonal wavelet denoising causes strong artifacts with increasing dimensionality of the transform, see Fig. 3d,e. 3D orthogonal wavelet denoising gives unacceptable results in terms of preserving the signal and removing the noise, see Fig. 3 (d). Visual comparison (Fig. 2,3,4) as well as the proposed quantitative measures show the potential of invariant wavelet transforms for denoising 3D data. For comparison we applied median filtering to the test data Fig. 3 (c). Although median filtering removes a considerable amount of noise it also tends to weaken the signal and is therefore of no use for our application.

### 4. CONCLUSIONS

The interpretation of electron tomographic reconstructions using rendering techniques is difficult due to the strong image noise. We were therefore looking for algorithms to remove noise in 3D data while preserving the signal. A direct extension of 1D wavelet denoising [2] to higher dimensions is not possible due to the lack of invariance, resulting in a weak signal representation and strong denoising artifacts. Steerable pyramid provides a well-suited tool for denoising 2D images. However, extending the technique to higher dimensions is rather difficult. We show for the wavelet representation the redundancy imposed by translation- and direction-invariance to be necessary for denoising 3D data. Thus, we demonstrate the applicability of the invariant wavelet representation for denoising 3D data. Furthermore, we propose a thresholding scheme for denoising data with an unknown signal-noise relationship.

## REFERENCES

- [1] R.R. Coifman and D.L. Donoho, "Translation-invariant de-noising", Technical Report no. 475, Department of Statistics, Stanford University, May 1995
- [2] D.L. Donoho, "Nonlinear wavelet methods for recovery of signals, images, and densities from noisy and incomplete data", American Mathematical Society, Different Perspectives on Wavelets, vol. 1, pp. 173-205, 1993
- [3] E.P. Simoncelli, W.T. Freeman, E.H. Adelson, D.J. Heeger, "Shiftable Multiscale Transforms", IEEE Transactions on Information Theory, vol. 38, no. 2, pp. 587-607, March 1992
- [4] T.P.Y. Yu, A. Stoschek, D.L. Donoho, "Translation- and Direction-Invariant Denoising of 2-D and 3-D Images", to appear in Proc. SPIE, Wavelet Applications in Signal and Image Processing V, vol. 2825, 1996
- [5] W.O. Saxton and W. Baumeister, "The correlation averaging of regularly arranged bacterial cell envelope protein" J. Microscopy, vol. 127, pp. 127-138, 1982
- [6] K. Dierksen, D. Typke, R. Hegerl, J. Walz, E. Sackmann, W. Baumeister, "Three-Dimensional Structure of Lipid Vesicles Embedded in Vitreous Ice and Investigated by Automated Electron Microscopy", Biophysical Journal, vol. 68, pp. 1416-1422, 1995

## ACKNOWLEDGMENTS

Thanks to D. Donoho (Stanford University) for discussion and help with the denoising. We are thankful to E. Simoncelli (University of Pennsylvania at Philadelphia) for providing a 6-orientation version of the steerable pyramid. Z. Cejka and R. Grimm (Max-Planck-Institute for Biochemistry) kindly provided the electron microscopy images. Thanks to G. Hauske (Technical University of Munich) for critical comments on the paper. This work was supported by Deutsche Forschungsgemeinschaft under contract no. HE 1404/4, US NIH grant NS14506 and the Antelman Fund.

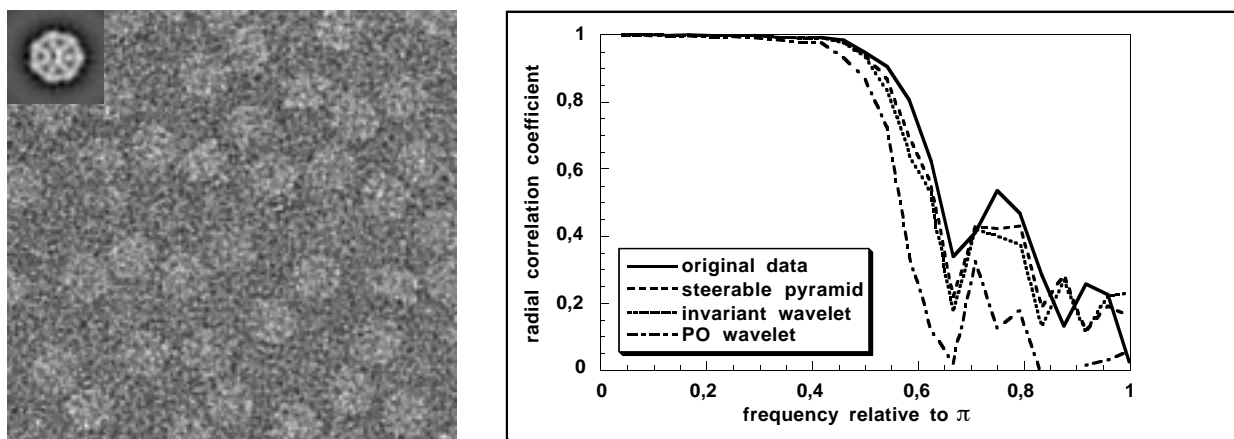


Figure 1: (left) Subframe of the test scene for denoising: low-dose, bright-field transmission electron micrograph of the proteasomal  $\alpha$ -subunit from *Thermoplasma acidophilum* [6], negative staining with uranyl acetate, fixation on carbon foil, pixelsize corresponds to 0.4 nm, superimposed the average of 3096 molecules; (right) radial correlation functions for original, 6-orientation steerable pyramid, translation- and rotation-invariant anisotropic wavelet, and periodized orthonormal wavelet (PO) denoised with Symmlet 8 wavelet kernel and soft thresholding for similar noise reduction

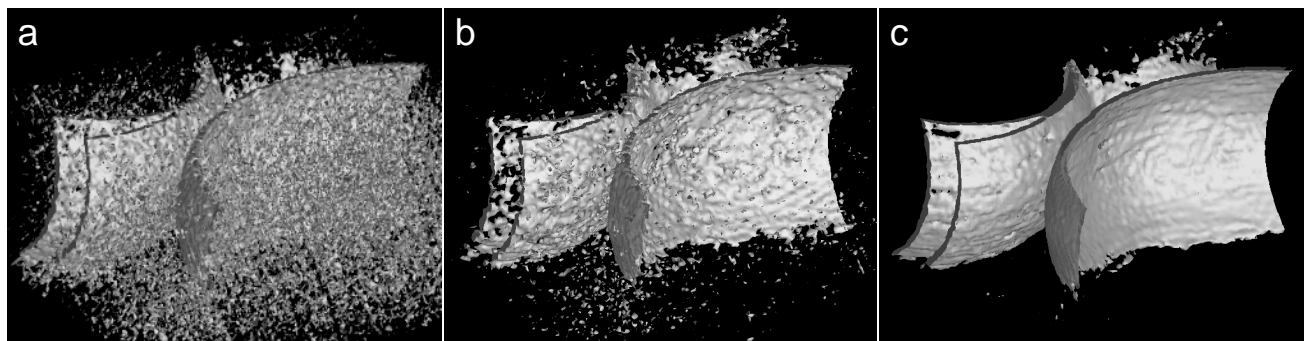


Figure 2: Isosurface representation from electron tomographic reconstruction of a DMPC vesicle, limited tilt angle  $-58^{\circ}/+58^{\circ}$ , 58 projections, vitreous ice embedding, width corresponds to ca. 100 nm, a) original data; b) orthogonal wavelet denoised; c) translation- and rotation-invariant anisotropic wavelet denoised; for (b, c) Symmlet 8 wavelet kernel and soft thresholding

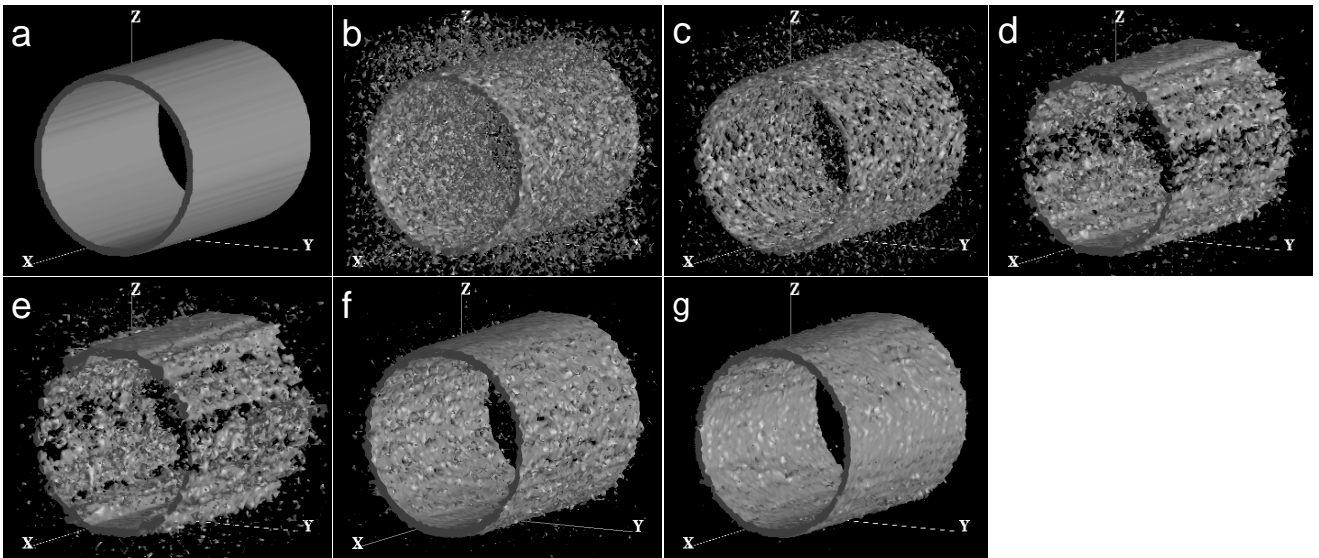


Figure 3: Isosurface representation of synthetic data (cube with 256x256x256 pixels) to be corrupted with white Gaussian noise  $\sigma=3$ ; a) original data; b) noisy data; c) median filtering d) pseudo-3D orthogonal wavelet denoised e) 3D orthogonal wavelet denoised; f) 6-orientation steerable pyramid pseudo-3D denoised, g) 3D translation-invariant anisotropic wavelet denoised; for (d ,e ,g) Haar wavelet kernel; for (d ,e ,f, g) soft thresholding

data	noise reduction	mean squared error	cross-correlation coefficient
noisy data	/	2.35	0.0756
median filtered	4.01	0.570	0.262
pseudo-3D orthogonal wavelet denoised	4.85	0.516	0.141
3D orthogonal wavelet denoised	4.81	0.421	0.114
6-orientation steerable pyramid denoised	4.61	0.420 *	0.183 *
3D translation-invariant wavelet denoised	8.26	0.251	0.252

Table 1: Noise reduction, mean squared error, and cross-correlation coefficient for the data in Fig. 3

\* Note: The steerable pyramid inherently does not provide a perfect reconstruction. However, the reconstruction error of the steerable pyramid was found to be negligible here.

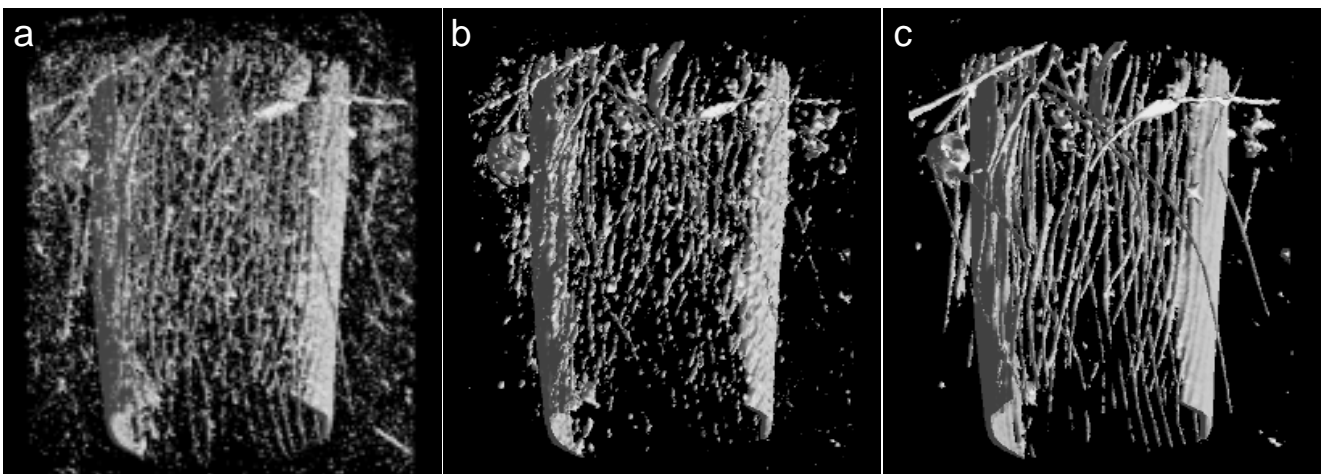


Figure 4: Isosurface representation from electron tomographic reconstruction of a DMPC vesicle with actin filaments, limited tilt angle  $-58^\circ/+58^\circ$ , 58 projections, vitreous ice embedding, diameter corresponds to ca. 100 nm, a) original data; b) orthogonal wavelet denoised; c) translation- and rotation-invariant anisotropic wavelet denoised; for (b, c) Symmlet 8 wavelet kernel and soft thresholding